Published in final edited form as:
J Magn Reson. 2008 April ; 191(2): 248–258. doi:10.1016/j.jmr.2007.12.015.

Correcting reaction rates measured by saturation-transfer magnetic resonance spectroscopy☆

Refaat E. Gabr[a,b], **Robert G. Weiss**[c], and **Paul A. Bottomley**[a,b,*]

[a] Division of MR Research, Department of Radiology, The Johns Hopkins University, JHOC 4221, Baltimore, MD 21287, USA

[b] Department of Electrical and Computer Engineering, The Johns Hopkins University, Baltimore, MD 21287, USA

[c] Division of Cardiology, Department of Medicine, The Johns Hopkins University, Carnegie 584, Baltimore, MD 21287, USA

Abstract

Off-resonance or spillover irradiation and incomplete saturation can introduce significant errors in the estimates of chemical rate constants measured by saturation-transfer magnetic resonance spectroscopy (MRS). Existing methods of correction are effective only over a limited parameter range. Here, a general approach of numerically solving the Bloch–McConnell equations to calculate exchange rates, relaxation times and concentrations for the saturation-transfer experiment is investigated, but found to require more measurements and higher signal-to-noise ratios than *in vivo* studies can practically afford. As an alternative, correction formulae for the reaction rate are provided which account for the expected parameter ranges and limited measurements available *in vivo*. The correction term is a quadratic function of experimental measurements. In computer simulations, the new formulae showed negligible bias and reduced the maximum error in the rate constants by about 3-fold compared to traditional formulae, and the error scatter by about 4-fold, over a wide range of parameters for conventional saturation transfer employing progressive saturation, and for the four-angle saturation-transfer method applied to the creatine kinase (CK) reaction in the human heart at 1.5 T. In normal *in vivo* spectra affected by spillover, the correction increases the mean calculated forward CK reaction rate by 6–16% over traditional and prior correction formulae.

Keywords

Saturation transfer; Magnetic resonance spectroscopy; Forward reaction rate; Chemical exchange; Creatine kinase

1. Introduction

Flux through energy-producing metabolic reactions is critical for cellular viability and fueling key cellular functions. Adenosine triphosphate (ATP) is the chemical energy currency for most cells in the body and the dynamic turnover of ATP can be probed non-invasively with

☆This work was supported by Grants RO1HL56882 and HL61912, and by the Donald W. Reynolds Foundation.

*Corresponding author. Address: Division of MR Research, Department of Radiology, The Johns Hopkins University, JHOC 4221, Baltimore, MD 21287, USA. Fax: +1 410 614 1977. E-mail address: bottoml@mri.jhu.edu (P.A. Bottomley).

phosphorus (^{31}P) magnetization-transfer magnetic resonance spectroscopy (MRS) techniques. The creatine kinase (CK) reaction:

$$\text{Phosphocreatine (Pcr)} + \text{Adenosine diphosphate (ADP)} + \text{H}^+ \leftrightarrow \text{ATP} + \text{creatine (Cr)},$$

is the prime short-term ATP reserve that serves to maintain constant ATP and ADP concentrations in the heart and may play a key role as an intracellular shuttle of high-energy phosphates between the mitochondria and sites of energy use in brain, skeletal muscle and heart [1]. In the failing heart, for example, abnormalities in CK flux in cardiomyopathies suggest an underlying energy supply defect [2-4]. Saturation-transfer MRS is an established method for measuring the CK reaction rate and flux *in vivo*, by selectively saturating one of the exchanging moieties, γ-ATP, and measuring the response in the reactant moiety, PCr.

In the standard two-site saturation-transfer experiment applied to two moieties A and B undergoing chemical exchange, the fractional reduction in the signal of A due to complete saturation of B, is equal to the pseudo-first order forward rate constant k in units of the apparent spin–lattice relaxation time of A, T_{1A}^{sat} [5],

$$kT_{1A}^{sat} = 1 - A_s/A_n \quad (1)$$

where A_s and A_n are the steady-state fully-relaxed magnetization of A in the presence (subscript s), and absence (subscript n), of a saturating irradiation applied to B, and

$$1/T_{1A}^{sat} = 1/T_{1A} + k \quad (2)$$

where T_{1A} is the "intrinsic T_1" of A. The simplified notation used here is summarized in Table 1. The determination of k then requires measurements of A_s, A_n and T_{1A}^{sat}. The relaxation rate constant T_{1A}^{sat} is commonly measured using standard progressive saturation [6], or, in humans using the more efficient four-angle saturation-transfer (FAST) method which uses a pulse repetition period, TR, much shorter than the spin–lattice relaxation times, T_1 [7].

The derivation of Eq. (1) assumes both perfect saturation of B and an absence of off-resonance, or spillover irradiation effects on A while saturating B [5]. The conventional way to account for any spillover effect is to perform a control saturation experiment where the saturation is applied to the other side of A from B at a frequency, ω_{RF}, of $2\omega_A - \omega_B$ where ω_A and ω_B are the resonant frequencies of A and B, respectively. The magnetization of A during this control experiment, A_c, is then substituted for A_n in Eq. (1), to yield a conventional k,

$$k_{conv}T_{1A}^{sat} = 1 - A_s/A_c. \quad (3)$$

By this means, the saturating field is supposed to have the same spillover effect on A during both the B saturation and the control experiments, thereby canceling the error via the ratio A_s/A_c. However, this procedure ignores the effects of chemical exchange and of spillover irradiation on B during the control experiment [8,9].

Errors in the reaction rate and relaxation times arising from off-resonance and incomplete saturation effects have been reported [6,10-12]. Strategies for correcting these errors have been suggested, which typically require additional acquisitions with the saturating irradiation

completely turned-off [8,9,13-15]. This includes a study by Kingsley and Monahan [13] in which existing and novel formulae for correcting k were compared in two models of proton (^{1}H) and phosphorus (^{31}P) chemical exchange. They found that no single formula could provide an accurate correction over all levels of saturating field strengths, but the more accurate candidates to replace Eq. (3) were the Horska–Spencer (HS) formula [9]:

$$k_{\mathrm{HS}} T_{1\mathrm{A}} = \frac{(\mathrm{A_c} - \mathrm{A_s})/\mathrm{A_n}}{(\mathrm{B_c} - \mathrm{B_s})/\mathrm{B_n} - (\mathrm{A_c} - \mathrm{A_s})/\mathrm{A_n}}; \tag{4}$$

and the Kingsley–Monahan (KM) formula (their Eq. (27))

$$k_{\mathrm{KM}} T_{1\mathrm{A}}^{\mathrm{sat}} = \frac{(\mathrm{A_c} - \mathrm{A_s})/\mathrm{A_n}}{(\mathrm{B_c} - \mathrm{B_s})/\mathrm{B_n}}. \tag{5}$$

The latter performed best in their study [13] when limited to a single specified set of parameters representing the expected value for the resonant frequencies, concentrations, relaxation times and reaction rate constants for the two models. However, variations in these parameters still resulted in large errors in the calculated k [7].

Consider for example, the ^{31}P MRS saturation-transfer experiment for measuring the kinetics of the CK reaction above. Chemical exchange between the PCr (site A), and the γ-ATP moiety (site B), is measured in a simulated standard saturation-transfer experiment using both progressive saturation and FAST methods as described below in Section 3. The relative errors in k obtained when using Eqs. (3)-(5) computed with a numerical evaluation of the Bloch–McConnell (BM) equations [16] for the CK reaction are plotted in Fig. 1 with typical parameters within the ranges listed in Table 2. The error contours reflect relative errors in k of over 30%, which vary considerably over the range of k and the applied saturating field strength, ω_1.

These potentially large errors motivated us to investigate new strategies for correcting the pseudo-first order forward CK reaction rate-constant measured with saturation transfer. While direct numerical solution of the BM equations for two-site chemical exchange might be considered a “gold standard” for accuracy, it nevertheless requires precise knowledge of a number of experimental measurements, which, due to the limited scan time of about an hour for localized *in vivo* human ^{31}P MRS at current signal-to-noise ratios (SNR), is often unavailable. Therefore, we introduce two new solutions which add correction terms to k derived from the KM formula, to cancel out the systematic errors evident in Fig. 1, using practical measurable quantities. We validate these corrections using computer simulations, and compare the effect of different correction formulae on real data from *in vivo* FAST localized ^{31}P MRS studies of the human heart.

2. Theory

2.1. The Bloch–McConnell (BM) equations

The BM equations [16] introduce a modification of the Bloch equations to describe the evolution of the magnetization M of chemically exchanging sites, A and B in a two-site system. During the application of a constant saturating RF field of strength ω_1 aligned with the x-axis of a frame of reference rotating at frequency ω_{RF}, the BM equations in matrix form are [7,8, 16]

$$\frac{\mathrm{d}}{\mathrm{d}t}\mathbf{M}=\mathbf{S}\mathbf{M}+\mathbf{C} \tag{6}$$

with $\mathbf{M} = (M_{Ax}\, M_{Ay}\, M_{Az}\, M_{Bx}\, M_{By}\, M_{Bz})^{T}$, $\mathbf{C} = (0\ 0\ M_{0A}/T_{1A}\ 0\ 0\ M_{0B}/T_{1B})^{T}$,

$$\mathbf{S}=\begin{pmatrix} -\frac{1}{T_{2A}}-k & \Delta\omega_{A} & 0 & k_{r} & 0 & 0 \\ -\Delta\omega_{A} & -\frac{1}{T_{2A}}-k & \omega_{1} & 0 & k_{r} & 0 \\ 0 & -\omega_{1} & -\frac{1}{T_{1A}}-k & 0 & 0 & k_{r} \\ k & 0 & 0 & -\frac{1}{T_{2B}}-k_{r} & \Delta\omega_{B} & 0 \\ 0 & k & 0 & -\Delta\omega_{B} & -\frac{1}{T_{2B}}-k_{r} & \omega_{1} \\ 0 & 0 & k & 0 & -\omega_{1} & -\frac{1}{T_{1B}}-k_{r} \end{pmatrix}$$

and where the superscript T denotes transposition; M_{0A} and M_{0B} are the fully relaxed equilibrium magnetization of A and B, respectively; $\Delta\omega_A = \omega_A - \omega_{RF}$, $\Delta\omega_B = \omega_B - \omega_{RF}$,($x$, y, z) are coordinate axes in the rotating frame; and $k_r = kM_{0A}/M_{0B}$ is the reverse reaction rate constant at equilibrium. The general solution of this equation is given by [7,11]:

$$\mathbf{M}(t)=\mathbf{e}^{\mathbf{S}t}\left(\mathbf{M}(t=0)+\mathbf{S}^{-1}\mathbf{C}\right)-\mathbf{S}^{-1}\mathbf{C} \tag{7}$$

Free precession in periods when the saturation field is turned-off, is similarly described by replacing **S** by a new matrix $\mathbf{F} = \mathbf{S}(\omega_1 = 0)$. Upon iterating periods of saturation and acquisition, the magnetization reaches a steady-state, and partial saturation occurs when the sequence repetition period, TR ~ T_1 of the exchanging species. The steady-state magnetization after the last acquisition pulse is given by:

$$\begin{aligned}\mathbf{M}= \quad & \mathbf{R}\left(\mathbf{I}-\mathbf{e}^{\mathbf{S}\cdot(\mathrm{TR}-\mathrm{TF})}\mathbf{e}^{\mathbf{F}\cdot\mathrm{TF}}\mathbf{R}\right)^{-1}\left[\left(\mathbf{e}^{\mathbf{S}\cdot(\mathrm{TR}-\mathrm{TF})}-\mathbf{I}\right)\mathbf{S}^{-1}\right. \\ & \left.+\,\mathbf{e}^{\mathbf{S}\cdot(\mathrm{TR}-\mathrm{TF})}\left(\mathbf{e}^{\mathbf{F}\cdot\mathrm{TF}}-\mathbf{I}\right)\mathbf{F}^{-1}\right]\mathbf{C}.\end{aligned} \tag{8}$$

Here TF is the time of free precession, **I** is a 6 × 6 identity matrix and **R** is a rotation matrix corresponding to an RF pulse with a flip angle α:

$$\mathbf{R}=\begin{bmatrix} 1 & 0 & 0 & 0 & 0 & 0 \\ 0 & \cos\alpha & -\sin\alpha & 0 & 0 & 0 \\ 0 & \sin\alpha & \cos\alpha & 0 & 0 & 0 \\ 0 & 0 & 0 & 1 & 0 & 0 \\ 0 & 0 & 0 & 0 & \cos\alpha & -\sin\alpha \\ 0 & 0 & 0 & 0 & \sin\alpha & \cos\alpha \end{bmatrix}.$$

2.2. Numerical solution of the BM equations

Using the BM equations above, the steady-state values of the magnetization of A and B resulting from the entire saturation-transfer experiment can be determined for the specified set of parameters. The standard saturation-transfer experiment involves a B-site saturation, a control-site saturation, and saturation-off sub-experiments [7]. The BM equations represent a nonlinear system whose analytical solution is unmanageable. However the problem is tractable with numerical approaches, as schematically shown in Fig. 2. By numerically inverting this

system (iteratively obtaining the input parameters from the output magnetization), spillover and/or incomplete saturation effects can be correctly accounted for, provided that a sufficient number of accurate measurements are available. Inverting the system yields estimates of the concentrations and relaxation times of A and B, in addition to *k*. The remaining inputs to this system include ω_1, ω_{RF}, the frequency separation between A and B and experiment-specific parameters such as the type of the saturation transfer experiment (progressive saturation, inversion recovery, FAST, etc) and the experimental parameters TR, TF, α, etc., while the output of the system is the measured steady-state magnetization of A and B.

Thus, the solution is formulated as a multidimensional nonlinear optimization problem. The nonlinear least-squares method is used to minimize the norm of the deviation of the outputs of Eq. (8) from the measured magnetization values, over the specified parameter space. We found that the alternative global search technique of simulated annealing [17] offered little improvement in accuracy in return for its increased computational load compared to the least squares approach. Restricting the search space using prior knowledge about the exchanging sites, such as the expected range of T_1 and T_2, was employed to hasten calculations and enhance solution stability.

Although numerical inversion can accurately solve the problems of off-resonance and incomplete saturation under many conditions, at least seven independent measurements are required to solve for M_{0A}, T_{1A}, T_{2A}, M_{0B}, T_{1B}, T_{2B}, and *k*. For accuracy, even more measurements are necessary when SNR is low. Unfortunately, the number of measurements provided by *in vivo* experiments is limited by the tolerable scan time, for example, in patient studies. In such cases, the numerical solution of the BM equations is sensitive to noise. We will illustrate the potential of applying this method in simulations involving the limited set of measurements that are routinely acquired in a FAST experiment, in addition to a standard saturation transfer experiment employing the progressive saturation method. The latter provides more measurements but is presently too time-consuming to be practical for localized saturation-transfer experiments in humans.

2.3. Correcting systematic errors in conventional formulae

An alternative solution to the spillover irradiation/incomplete saturation problem is to correct for the systematic errors in *k* when calculated from one of the conventional formulae. Systematic errors in *k* are determined from an accurate simulation of the BM equations and the results either saved to a look-up table for post-correction, or fitted with a suitable basis function (e.g. a polynomial) to obtain a closed-form correction formula. The latter is feasible if the systematic error is smooth enough to be accurately modeled by the basis functions within acceptable residual errors, after correction. Hence, a conventional formula with a smooth error surface in *k* over a realistic parameter space is desired. This condition is satisfied by the KM formula, Eq. (5), and is presented in Section 4.

While all input parameters to the BM equations affect the calculated *k*, the most influential parameters are the actual value of *k*, the spillover degree as indexed by the ratio of the saturating field strength to the frequency separation between the two sites, $\omega_1/|\omega_A - \omega_B|$ [8], and TR. Since TR is usually fixed as a user-defined parameter for the FAST protocol, we will neglect its change. Subtracting a term Δk that depends on the relevant parameters, we obtain a corrected value of *k*, k_{corr}:

$$k_{corr} = k_{KM} - \Delta k\left(k_{KM}, \omega_1 / \left|\omega_A - \omega_B\right|\right) \quad (9)$$

Using polynomial basis functions, the correction is

$$k_{\mathrm{corr}}=k_{\mathrm{KM}}-P_k\left(k_{\mathrm{KM}}\right)P_\omega\left(\omega_1/\left|\omega_{\mathrm{A}}-\omega_{\mathrm{B}}\right|\right) \tag{10}$$

where P_k and P_ω are second-order polynomials in their arguments. A second-order polynomial was found to give acceptable error levels while only minor improvements were achieved with higher orders. The correction term Δk is fitted to the systematic errors in k_{KM} over the ranges of the parameters listed in Table 2 using the method of least squares. The polynomial factors that minimize the error in k are given in Table 3 where the factors a_1, a_2 and a_3 are the coefficients of the quadratic polynomial $P(x) = a_1x^2 + a_2x + a_3$.

A practical problem with this solution is that the saturating field strength experienced by the exchanging species, ω_1, must be known. However, in general, ω_1 differs from the specified transmitter power. For example, most ^{31}P MRS is performed with surface coil excitation [2, 4].In these cases ω_1 is spatially-dependent and not easily determinable. In practice, the saturating field strength is manually adjusted as a fraction of a maximum allowed power, until the saturation of B appears satisfactory. In this situation, the spillover irradiation factor, $\omega_1/|\omega_{\mathrm{A}}-\omega_{\mathrm{B}}|$ should be replaced by a suitable measure such as $Q = \mathrm{A_c}/\mathrm{A_n}$ [7] which may vary spatially. The correction formula is then:

$$k_{\mathrm{corr}}=k_{\mathrm{KM}}-P_k\left(k_{\mathrm{KM}}\right)P_Q\left(Q\right) \tag{11}$$

where P_Q is a second-order polynomial in Q. The optimal polynomial factors in this case are given in Table 4, with a schematic of their derivation included in Fig. 2.

3. Methods

3.1. Simulations

The proposed correction methods are evaluated for a simulated CK reaction probed by two standard ^{31}P saturation-transfer methods. The first is a conventional saturation-transfer experiment with progressive saturation to measure the apparent $T_{1\mathrm{A}}$ $T_{1\mathrm{A}}^{\mathrm{sat}}$. The progressive saturation portion includes acquisitions with TR = 0.6, 1, 2, 3, 4, 8, 12 and 16 s, with the B-site saturated. In addition, acquisitions with the control-site saturated, and with the saturation turned-off, are both recorded at TR = 16 s. The FAST experiment incorporates the dual-angle method for measuring $T_{1\mathrm{A}}^{\mathrm{sat}}$ [18]. In FAST, A is measured twice with B saturated, and twice with control irradiation (at $2\omega_{\mathrm{A}}-\omega_{\mathrm{B}}$) using two different (adiabatic) flip-angles, 60° and 15° at each site and TR = 1 s [7]. An additional 60° saturation-off experiment is performed at the same TR. The values of ω_1, the concentration ratio $M_{0\mathrm{A}}/M_{0\mathrm{B}}$, and the relaxation constant $T_{1\mathrm{A}}$ are allowed to vary over the ranges listed in Table 2, which also lists the fixed model values. All these values are consistent with existing data from heart and brain [7,19-21].

The entire progressive saturation and FAST experiments are simulated using the steady-state equations above (Eq. (8)), with Matlab (The MathWorks, Natick, MA). The relative error in k, $(k_{\mathrm{calculated}}-k_{\mathrm{true}})/k_{\mathrm{true}}$ where k_{true} is the input value of k in the range, is calculated for the conventional formula, Eq. (3), the HS formula, Eq. (4), the KM formula, Eq. (5), the numerical inversion method, and the new correction formulae provided here in Eqs. (10) and (11). For the numerical inversion method, 12 measurements are used in the progressive saturation method which are the partially-saturated magnetization values of A for the B-site saturation case at the eight different TR values in addition to the magnetization of A and B in the control and the saturation-off experiments. For FAST, only eight measurements are used to estimate the seven unknown variables. These are the partially-saturated magnetization values of A and

B measured at the two different flip angles (60° and 15°) with B- and control-site saturation, which are all potentially available from a FAST experiment followed by an experiment in which no saturation is applied at a flip angle of 60° [7,19]. The simulations are done over two ranges of k: a broad range of $0.05 \leqslant k \leqslant 1.0$ for general applications; and, to improve accuracy for *in vivo* cardiac FAST applications, a physiological range of $0.1 \leqslant k \leqslant 0.5$ [4], denoted FAST*. Note that the magnetization of B in the B-saturation experiment, B_S, which corresponds to γ-ATP in the presence of saturation, cannot be reliably measured when SNR is low, as is typical of *in vivo* studies. It is therefore set to zero in all calculations. In this case Kingsley–Monahan's Eq. (27) reduces to their Eq. (34), and the HS equation reduces to Eq. (33) in the same Ref. [13]. As noted [13], these two equations tend to underestimate k.

To determine the effect of noise on k for each correction formula, a *Monte Carlo* analysis is performed for the FAST method with PCr SNR values of 20–50 as measured on the 15° acquisition recorded with γ-ATP saturated, and $n = 100$ trials. This analysis yields two measures of accuracy: (i) the difference between the mean corrected value and the true value, or bias; and (ii) the standard deviation (SD) of the corrected k value, or scatter.

3.2. Experiments

We applied the new correction to ^{31}P MRS data available from prior studies of the human heart using the FAST method with one-dimensional chemical shift imaging (1D-CSI) localization, and a 1.5-T whole-body GE Signa scanner (Milwaukee, WI) system [4,7]. All experiments were performed using 4-ms BIRP adiabatic excitation pulses [7]. As in the simulations, the FAST method was applied at TR = 1 s, with four acquisitions employing flip angles of 15° and 60°, and with γ-ATP and control saturation applied at ±2.7 ppm relative to PCr. A fifth ^{31}P MRS data set was acquired with a 60° pulse and no selective saturation to measure Q. The total duration of the complete image-guided localized MRS exam was about 60–75 min. Continuous RF applied at 2% of the maximum ^{31}P MRS power level, provided the chemical-selective saturating field strength of 5–10 Hz over the sensitive volume of the detector coil. The saturating pulse was switched-off for TF = 180 ms during BIRP excitation and data acquisition. The pulse amplitude was set at the minimum level required to provide complete saturation of γ-ATP at visual inspection of surface coil ^{31}P spectra acquired during set-up of each study. All ^{31}P data acquisitions were preceded by a train of dummy excitations lasting 16–20 s, to establish steady-state equilibrium. All subjects provided informed consent, and these studies were approved by our institutional review board.

The effect of applying the conventional formula, the HS formula, the KM formula, and the correction formula in Eq. (11) on the reaction rate k was first calculated using the same 57 FAST data sets acquired from different cardiac slices in 18 healthy subjects. The numerical inversion method and Eq. (10) were excluded from the comparison because the experiments did not provide an accurate measure of ω_1. The analysis was performed three ways. First, because none of the correction formulae are strictly applicable to spectra with measured $Q > 1$, these data were excluded, resulting in a sample of 38 normal 1D-resolved cardiac spectra from 14 healthy subjects. $Q > 1$ is not meaningful, but arises when true $Q \sim 1$ and SNR is low. Second, all data were included but we set $Q = 1$ when $Q > 1$ was measured. Third, all data were included with their actual measured Qs.

Next, the effect of varying both the experimental Q and k on the magnitude of the correction resulting from the application of the different correction formulae was investigated. In order to provide as wide a range of experimental Q and k values as possible, this analysis used the 38 cardiac spectra from the 14 healthy subjects above, along with 75 spectra from 34 patients with hypertrophic or dilated cardiomyopathies [4,7] that satisfied the $Q \leqslant 1$ criterion. Details of the patient selection criteria and the physiological interpretations of these data are provided elsewhere [4,7], and are beyond the scope of the present paper. Several typical localized

cardiac ^{31}P MRS spectra from a FAST study of a patient performed at 1.5 T, are shown in Fig. 3.

4. Results

4.1. Simulations

The relative errors in the forward reaction rate constant calculated by different methods, as compared to the input k, are listed in Table 5. Of the pre-existing formulae Eqs. (3)-(5), the smallest range of errors in k for both progressive saturation and FAST, results from using the KM formula, justifying its choice here as a basis for correction in Eqs. (10) and (11). In applying the different correction methods to progressive saturation, the smallest errors are obtained by numerical inversion. The two proposed correcting formulae in Eqs. (10) and (11) perform similarly to the KM formula. Numerical inversion has the least bias and has 2–6 times less scatter (SD) in the error than the conventional, the HS, and the KM formulae, over the specified range of conditions. Our new Eqs. (10) and (11) exhibit negligible bias and up to four times lower SD than these formulae.

For FAST, the smallest errors are obtained with the two new correcting formulae, Eqs. (10) and (11). Our new Eq. (10), shows no bias and has on average 6–7 times lower scatter than the conventional, the HS, and the KM formulae, while new Eq. (11) has a negligible bias with a 4- to 5-fold lower SD of the error. The numerical inversion method also shows negligible bias and has 2–3 times less scatter than the traditional formulae, but the errors are nevertheless, still about double those from Eqs. (10) and (11).

The errors in k for the conventional, the HS, and the KM formulae as a function of k and ω_1 at $T_{1A} = 6$ s and $M_{0A}/M_{0B} = 1.5$, are shown in Fig. 1. Of the pre-existing Eqs. (3)-(5), KM fares best for progressive saturation, but for FAST, the conventional Eq. (3) is better than Eqs. (4) and (5) over the parameter space. Plots of the errors after applying the numerical inversion method and the correction formulae in Eqs. (10) and (11) are shown in Fig. 4 for the same parameters. Compared to Fig. 1, Fig. 4 shows a major improvement in accuracy using any of the three proposed corrections.

Table 5 also shows that the errors over the physiological range $0.1 \leqslant k \leqslant 0.5$ are smaller, although the reduction in error is not the same for all methods. The conventional formula provides significantly improved k estimation both in terms of bias and scatter, over the reduced range. This is mainly due to large errors at the very low and the very high values of k evident in Fig. 1. The KM formula, the numerical inversion method and Eqs. (10) and (11) show a moderate reduction in the scatter of error, while the HS formula shows the least improvement. Both Eqs. (10) and (11) retain their superior performance over the physiologic range of k in the human heart.

The results of the *Monte Carlo* analysis are plotted in Fig. 5. These show that the new Eq. (11) performs better than prior correction methods in the presence of noise, and that use of k_{conv} appears to be a better option than k_{HS} and k_{KM}, at least over the physiological range, $0.1 \leqslant k \leqslant 0.5$.

4.2. Effect on experimental data

The forward reaction rate constants k, calculated from the different correction formulae as applied to healthy subjects, are listed in Table 6. These are the mean k from all subjects, after averaging the slices for each subject. With the $Q > 1$ data excluded, the correction provided by Eq. (11) results in a 6% higher estimate of k compared with the conventional formula (0.36 s^{-1} vs. 0.34 s^{-1}). Both the HS and the KM formulae yield lower values than the conventional formula (0.31 and 0.32 s^{-1} vs 0.34 s^{-1}), consistent with that seen previously in muscle [7] and

in simulations [13]. These differences are all statistically significant (Table 6). The mean k values computed with Eq. (11) are not significantly affected by including data with $Q > 1$ either as is, or after setting measured Q values that are greater than one, equal to one.

The percentage adjustment to k_{conv} by the different correction formulae are plotted in Fig. 6 as a function of k_{conv} and Q, with the second-order best-fit lines overlaid. The corrections to k_{conv} by both the HS and the KM formulae depend significantly on the spillover factor, Q, while Eq. (11) depends less on Q, than on k_{conv}. This is consistent with Fig. 1 which shows that errors in k_{conv} depend more on k than on ω_1, for which Q is a proxy, as compared with k_{HS} and k_{KM} which are more sensitive to ω_1 (Fig. 1). Note that while use of Eq. (11) alters the mean values as noted above, the significant differences between heart disease patients and healthy subjects reported earlier [3,4], are preserved.

5. Discussion

We have introduced three methods to correct the reaction rate constant for spillover irradiation effects. The simulations show that for the progressive saturation method, numerical solution of the BM equations performs best while for FAST, the formula in Eq. (10) performs best over the specified parameter space (Table 2). For the traditional formulae, k_{conv}, k_{HS} and k_{KM}, a large bias is evident (Table 5) and the worst errors are as large as 70%, 36% and 18% for the progressive saturation method, and as large as 40%, 34% and 27% for FAST, respectively. The new formulae show negligible bias and reduce the maximum errors by about 3-fold and the SD of the error by about 4-fold for both a progressive saturation/saturation transfer and a FAST experiment, over a wide range of parameters that are realistic for ^{31}P MRS of the CK reaction in the heart, or even the brain, *in vivo* [20,21].

In FAST studies of CK flux in human hearts, the proposed correction in Eq. (11) produces mean k values that are 6% higher than those of the conventional formula, and 13–16% higher than the KM and the HS formulae, which have been applied in the past (Table 6). Indeed, Table 6 shows that for these cardiac studies, using the conventional formula may be more accurate than using either the HS or the KM formulae. Both the HS and KM formulae are more sensitive than the conventional formula to the spillover extent (ω_1) for FAST (Fig. 1). The KM formula outperforms the conventional formula for a conventional saturation-transfer/progressive-saturation experiment for which it is intended. The correction provided in Eq. (11), while relatively small (Table 6), is nevertheless significant for the assessment of CK ATP energy supply in absolute terms, which, in turn, is important for comparisons among various disease states from different studies as well as comparisons of this metabolic rate with other metabolic rates [3,4].

The first correction method investigated here, the numerical solution of the BM equations, has the potential to estimate all of the variables in a chemically exchanging system and to provide better estimates for k than existing approaches (Table 5). However, for FAST, the numerical inversion method performs worse than the corrections provided by Eqs. (10) and (11). This is because the numerical inversion jointly estimates all of the relaxation and concentrations of the two exchanging sites in addition to the reaction rate constant. The joint estimation is numerically more sensitive, especially when the number of measurements is as small as in FAST (eight measurements). This problem could be ameliorated by collecting more measurements and/or by measuring rather than estimating some of the parameters. However, both of these solutions are not really practical due to the limited scan time of patient studies, and the low SNR endemic to localized ^{31}P MRS. In addition, both the numerical inversion method and Eq. (10), require measurements of ω_1, which, as noted, is not easily determined if the saturating field is non-uniform, such as with surface coils. This prompted our introduction of Q as a practical, measurable proxy.

The proposed correction in Eq. (11) accounts for variations in k and Q, which are the largest contributors to the error in k computed from the conventional formula. However, it is straightforward to extend the correction function to include other variables. For example, changes in TR which were not considered here because TR is fixed or known, can easily be added to Eq. (11). Note also that while Eq. (11) successfully reduces the error in k, the P_Q term in the correction factor does not vanish and the formula does not reduce to the conventional formula (Eq. (1)) when spillover vanishes ($Q = 1$), even though the difference is relatively small. This is because there will always be some degree of incomplete saturation if spillover is minimized for the ^{31}P CK experiment at 1.5 T. In this case, the conventional formula is still an approximation that neglects the systematic error resulting from ignoring chemical exchange during the control experiment (quantified by the P_k term). It must also be remembered that optimization of the correction polynomials is performed for specific ranges of saturating field strength ($15 \leqslant \omega_1 \leqslant 63$ rad s^{-1}) and frequency separation (440 rad s^{-1} between PCr and γ-ATP at 1.5 T). In this regime, optimization of the saturation pulse is a difficult balance between incomplete saturation and excessive spillover, the effect of which is manifest in the range of empirical values seen in Q in Fig. 6.

The ^{31}P MRS simulations and experiments in this work focus on the CK reaction, which is of interest to *in vivo* studies as a source of cellular energy and as a buffer to maintain ATP and ADP relatively constant [1-4]. While we provide an analysis of a conventional saturation-transfer experiment, in practice we have found that, to date, only the FAST protocol is efficient enough for performing spatially localized human cardiac studies within tolerable scan times at 1.5 T [4,7]. Even so, both scan-time and SNR are at a premium in such studies, and the accuracy of the calculation of k would certainly improve if more measurements and/or data with better SNR could be practically acquired. Indeed, there are alternative methods of measuring reaction rates such as 1D or 2D exchange spectroscopy (EXSY) [10,22-24] that do not use chemical-selective irradiation and hence do not suffer from spillover effects. However, combining 1D spatially localized *in vivo* ^{31}P MRS with 1D or 2D EXSY, leads to impractical patient scan times, especially where fully-relaxed acquisitions are required [10], these being avoided by FAST. For saturation-transfer methods, the correction approaches described herein can be extended to proton spectra, other field strengths, and other protocols, requiring only re-calculation of the polynomial fitting coefficients for the new range of fitting parameters and available measurements.

In conclusion, we have introduced new solutions to the problems of irradiation spillover during the saturation-transfer experiment. These solutions provide corrections that significantly reduce errors in the calculated forward reaction rate constants in the practical implementation of ^{31}P MRS to measure CK reaction kinetics, and can be developed for other reaction systems as well.

References

1. Wallimann T. Bioenergetics. Dissecting the role of creatine kinase. Curr. Biol 1994;4(1):42–46. [PubMed: 7922310]
2. Ingwall JS, Weiss RG. Is the failing heart energy starved? On using chemical energy to support cardiac function. Circ. Res 2004;95(2):135–145. [PubMed: 15271865]
3. Weiss RG, Gerstenblith G, Bottomley PA. ATP flux through creatine kinase in the normal, stressed, and failing human heart. Proc. Natl. Acad. Sci. USA 2005;102(3):808–813. [PubMed: 15647364]
4. Smith CS, Bottomley PA, Schulman SP, Gerstenblith G, Weiss RG. Altered creatine kinase adenosine triphosphate kinetics in failing hypertrophied human myocardium. Circulation 2006;114(11):1151–1158. [PubMed: 16952984]
5. Gadian, DG. Nuclear Magnetic Resonance and its Applications to Living Systems. Clarendon Press; Oxford: 1982.

6. Horska A, Spencer RGS. Measurement of spin–lattice relaxation times and kinetic rate constants in rat muscle using progressive partial saturation and steady-state saturation transfer. Magn. Reson. Med 1996;36(2):232–240.
7. Bottomley PA, Ouwerkerk R, Lee RF, Weiss RG. Four-angle saturation transfer (FAST) method for measuring creatine kinase reaction rates in vivo. Magn. Reson. Med 2002;47(5):850–863. [PubMed: 11979563]
8. Baguet E, Roby C. Off-resonance irradiation effect in steady-state NMR saturation transfer. J. Magn. Reson 1997;128(2):149–160. [PubMed: 9356270]
9. Horska A, Spencer RGS. Correctly accounting for radiofrequency spillover in saturation transfer experiments: application to measurement of the creatine kinase reaction rate in human forearm muscle. Magn. Reson. Mater. Phys 1997;5(2):159–163.
10. Kuchel PW. Spin-exchange NMR spectroscopy in studies of the kinetics of enzymes and membrane transport. NMR Biomed 1990;3(3):102–119. [PubMed: 2201390]
11. Spencer RGS, Fishbein KW. Measurement of spin–lattice relaxation times and concentrations in systems with chemical exchange using the one-pulse sequence: breakdown of the Ernst model for partial saturation in nuclear magnetic resonance spectroscopy. J. Magn. Reson 2000;142(1):120–135. [PubMed: 10617442]
12. Ouwerkerk R, Bottomley PA. On neglecting chemical exchange effects when correcting in vivo (31) P MRS data for partial saturation. J. Magn. Reson 2001;148(2):425–435. [PubMed: 11237649]
13. Kingsley PB, Monahan WG. Corrections for off-resonance effects and incomplete saturation in conventional (two-site) saturation-transfer kinetic measurements. Magn. Reson. Med 2000;43(6):810–819. [PubMed: 10861875]
14. Kingsley PB, Monahan WG. Effects of off-resonance irradiation, cross-relaxation, and chemical exchange on steady-state magnetization and effective spin-lattice relaxation times. J. Magn. Reson 2000;143(2):360–375. [PubMed: 10729261]
15. Kingsley PB, Monahan WG. Correcting for incomplete saturation and off-resonance effects in multiple-site saturation-transfer kinetic measurements. J. Magn. Reson 2000;146(1):100–109. [PubMed: 10968962]
16. McConnell HM. Reaction rates by nuclear magnetic resonance. J. Chem. Phys 1958;28(3):430–431.
17. Laarhoven, PJM.; Aarts, EHL. Simulated Annealing: Theory and Applications. Kluwer Academic Publishers; Norwell, MA, USA: 1987.
18. Bottomley PA, Ouwerkerk R. The dual-angle method for fast, sensitive T1 measurement in vivo with low-angle adiabatic pulses. J. Magn. Reson. B 1994;104(2):159–167.
19. Bottomley PA, Ouwerkerk R. Optimum flip-angles for exciting NMR with uncertain T1 values. Magn. Reson. Med 1994;32(1):137–141. [PubMed: 8084230]
20. Bottomley PA, Hardy CJ. Mapping creatine kinase reaction rates in human brain and heart with 4 tesla saturation transfer ^{31}P NMR. J. Magn. Reson 1992;99(2):443–448.
21. Cadoux-Hudson TA, Blackledge MJ, Radda GK. Imaging of human brain creatine kinase activity in vivo. FASEB J 1989;3(14):2660–2666. [PubMed: 2629743]
22. Perrin CL, Gipe RK. Multisite kinetics by quantitative two-dimensional NMR. J. Am. Chem. Soc 1984;106(14):4036–4038.
23. Kuchel PW, Bulliman BT, Chapman BE, Mendz GL. Variances of rate constants estimated from 2D NMR exchange spectra. J. Magn. Reson 1988;76(1):136–142.
24. Bulliman BT, Kuchel PW, Chapman BE. Overdetermined one-dimensional NMR exchange analysis: a 1D counterpart of the 2D EXSY experiment. J. Magn. Reson 1989;82(1):131–138.

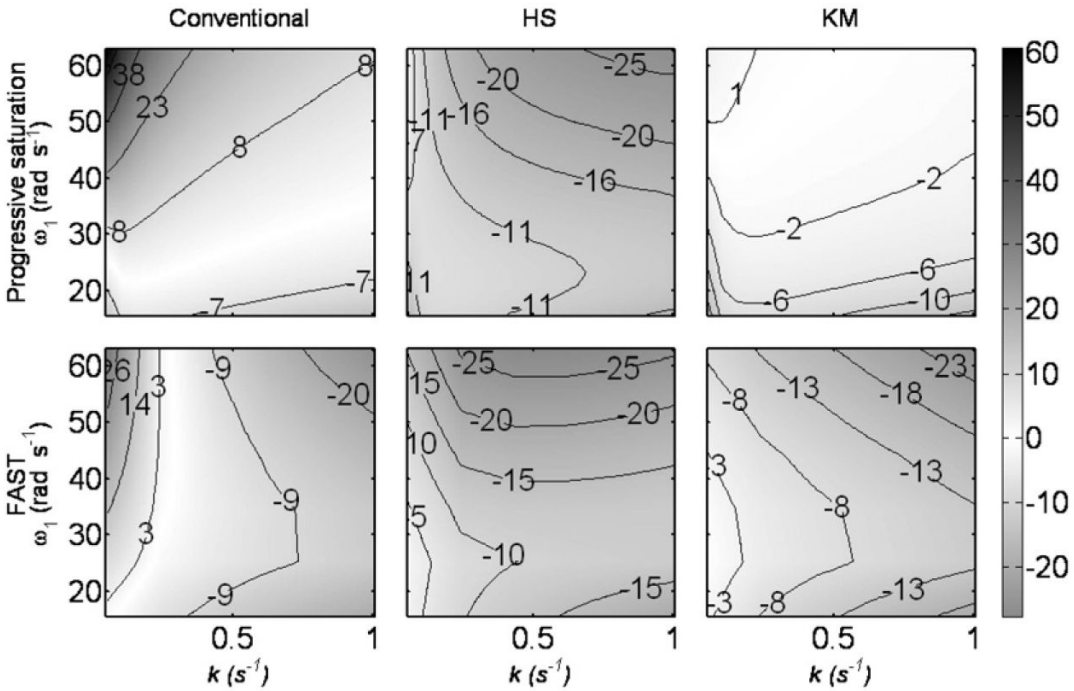

Fig. 1.

Percent error in the estimated value of the reaction rate constant k for simulated ^{31}P MRS saturation-transfer experiments of the CK reaction using the standard progressive saturation method (top) and the FAST method (below) as a function of ω_1 and k. The value of k is calculated using the conventional equation (3), the Horska–Spencer (HS) equation (4) and the Kingsley–Monahan (KM) equation (5) for T_{1A} = 6 s and M_{0A}/M_{0B} = 1.5. Errors are depicted both as contours and by the gray scale (right).

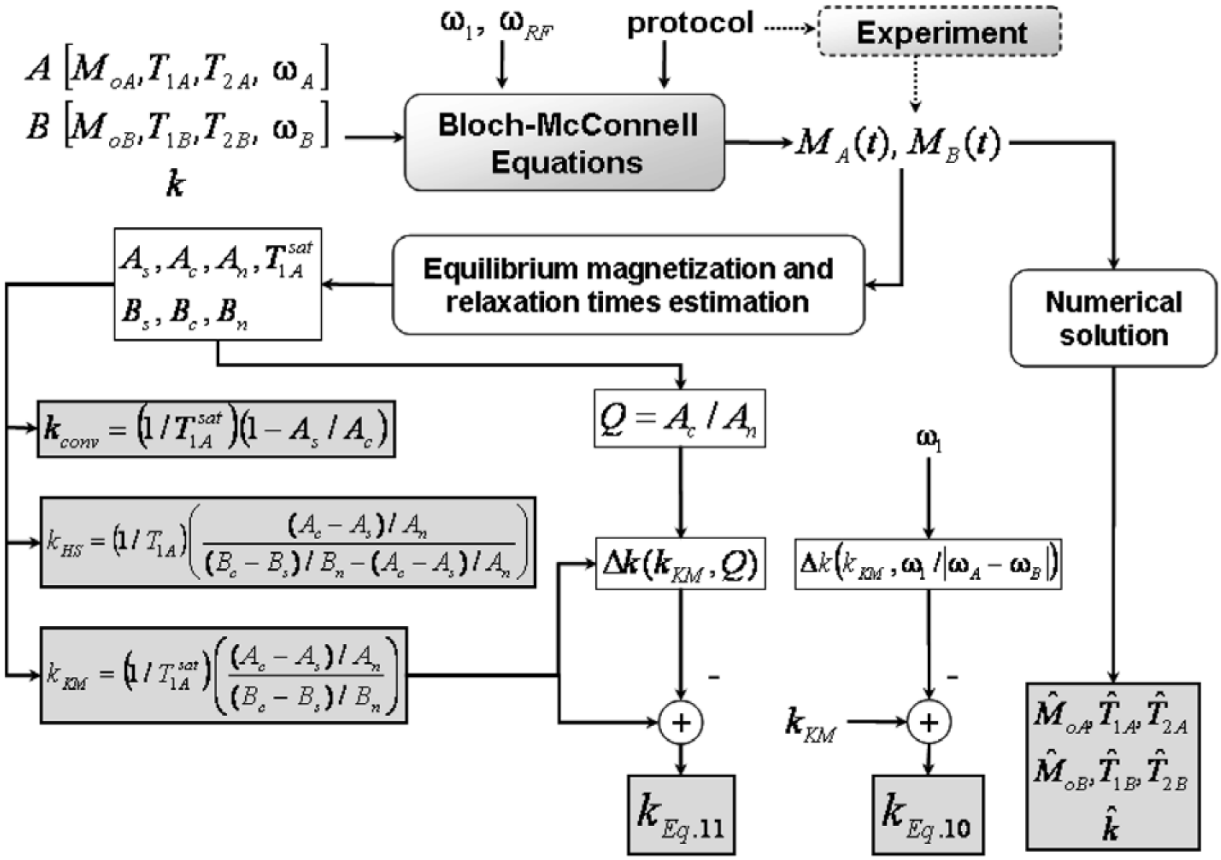

Fig. 2.

Correction strategies for *k* in steady-state saturation transfer experiments involving two-site chemical exchange. The parameters for each species are fed to the BM equations, from which the partially-saturated magnetizations are derived for a given experimental protocol. The fully-relaxed magnetizations and T_1's are estimated and used to compute the *k*s by the various correction equations, in the presence of spillover irradiation. A direct numerical solution is also computed.

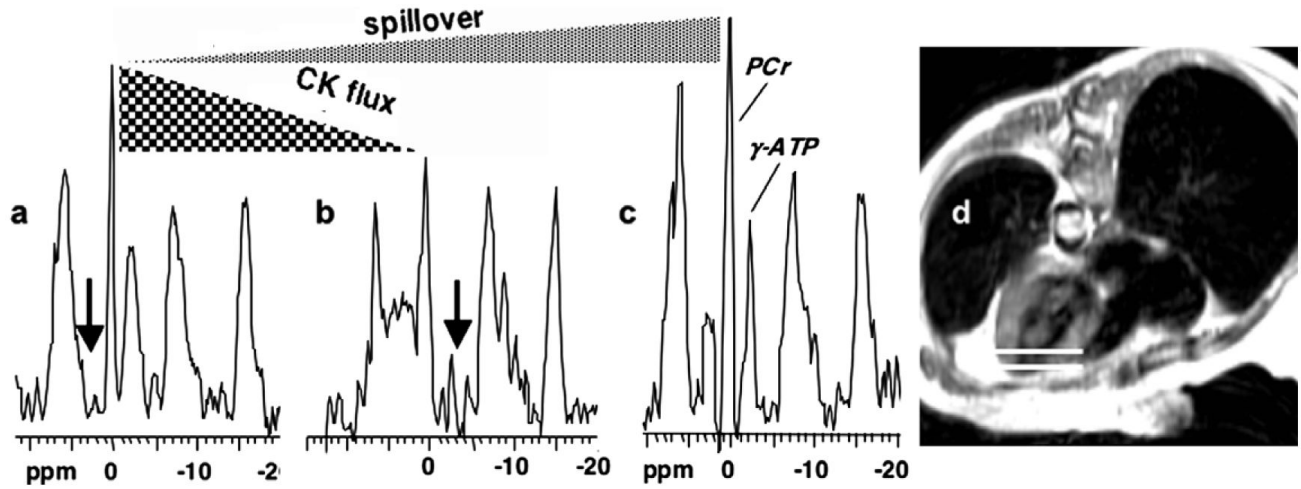

Fig. 3.

Typical ^{31}P MRS spectra (a–c) of an exemplary 1-cm slice in the anterior myocardium (d; annotated with horizontal white lines) extracted from a FAST CK flux study of a 55-year-old woman with New York Heart Association Class I–II heart failure at 1.5 T [3,4]. (a,b) Two of the four FAST acquisitions excited with a 60° pulse and control saturation (a; vertical arrow), and with γ-ATP saturated (b). The reduction in PCr signal between (a) and (b) is due to CK flux in the heart. ^{31}P Spectrum (c) is acquired with no saturation, to measure PCr concentration, and to measure the spillover effect. The reduction in PCr signal between (a) and (c) is due to spillover irradiation, and is quantified by *Q*.

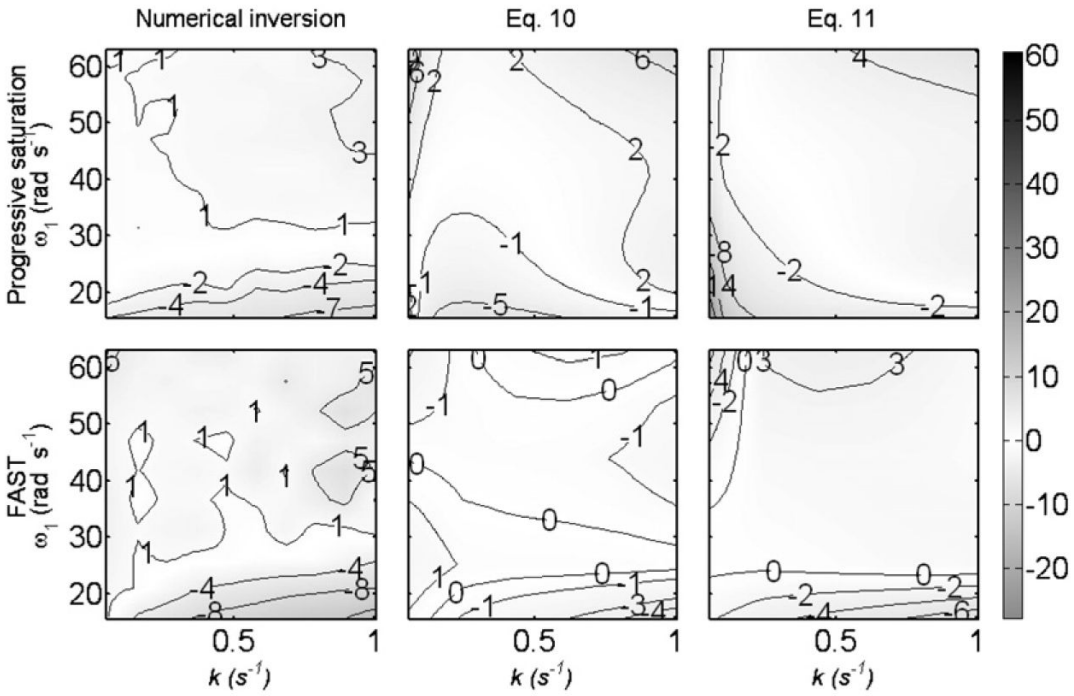

Fig. 4.

Percent error in the estimated value of the reaction rate constant k for ^{31}P-simulated saturation-transfer experiments of the CK reaction using the standard progressive-saturation method and the FAST method as a function of ω_1 and k. The value of k is calculated using the numerical inversion method, Eqs. (10) and (11) for T_{1A} = 6 s and M_{0A}/M_{0B} = 1.5. Errors are depicted both as contours and by the same gray scale used in Fig. 1.

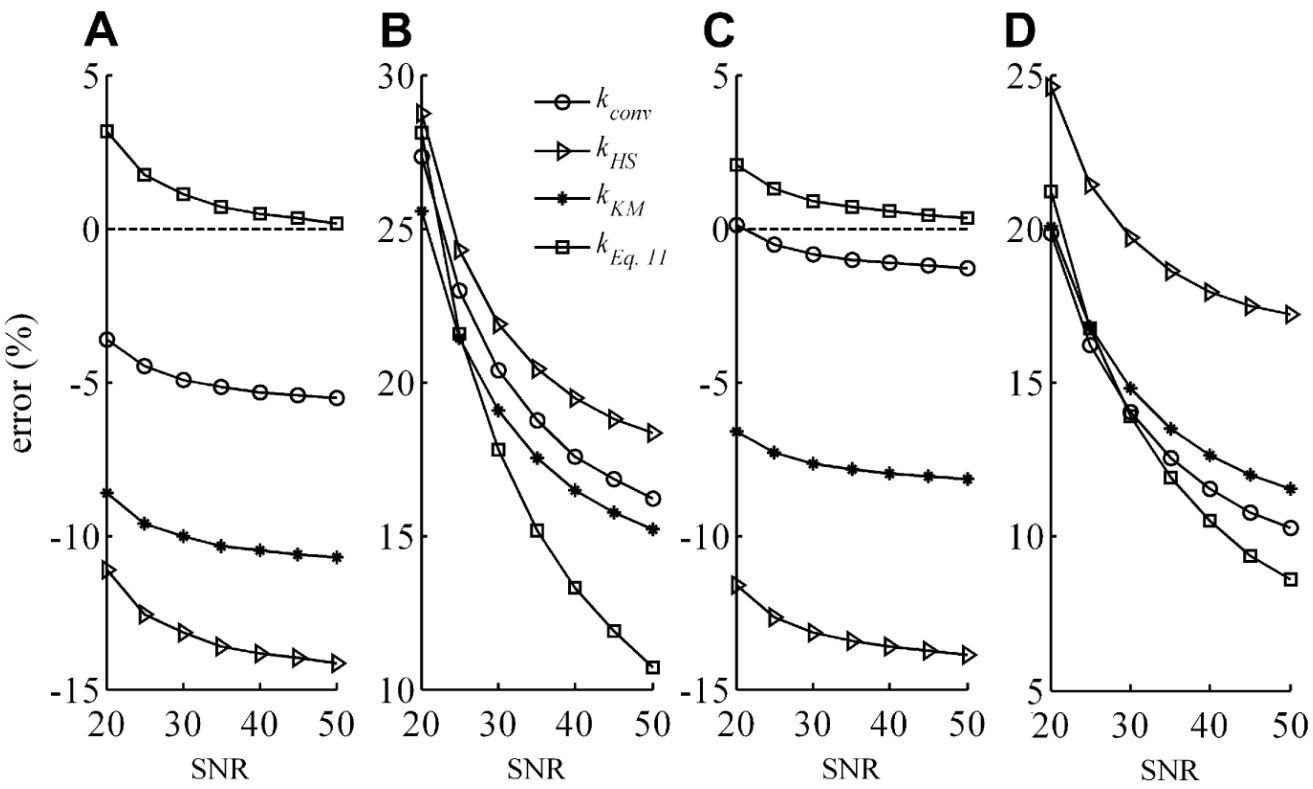

Fig. 5.

Percent mean error or bias (A,C) and scatter in the error or SD (B,D) in the estimated value of the reaction rate constant k for simulated ^{31}P FAST experiments of the CK reaction as a function of the SNR levels for the PCr signal in the 15° γ-ATP-saturation experiment, as determined by a 100-run Monte Carlo simulation. The value of k over both the wide range ($0.05 \leqslant k \leqslant 1.0$; (A,B); $k_{\text{Eq. (11)}}$ using FAST coefficients from Table 4), and the more restrictive physiological range ($0.1 \leqslant k \leqslant 0.5$; (C,D); $k_{\text{Eq. (11)}}$ using FAST* coefficients), was sampled by 6 points, as were T_{1A}, ω_1, and M_{0A}/M_{0B} over the ranges listed in Table 2. For each run, the mean error in k was calculated for the 6^4 combinations of variables in the range, and the mean and SD error for the 100 runs reported.

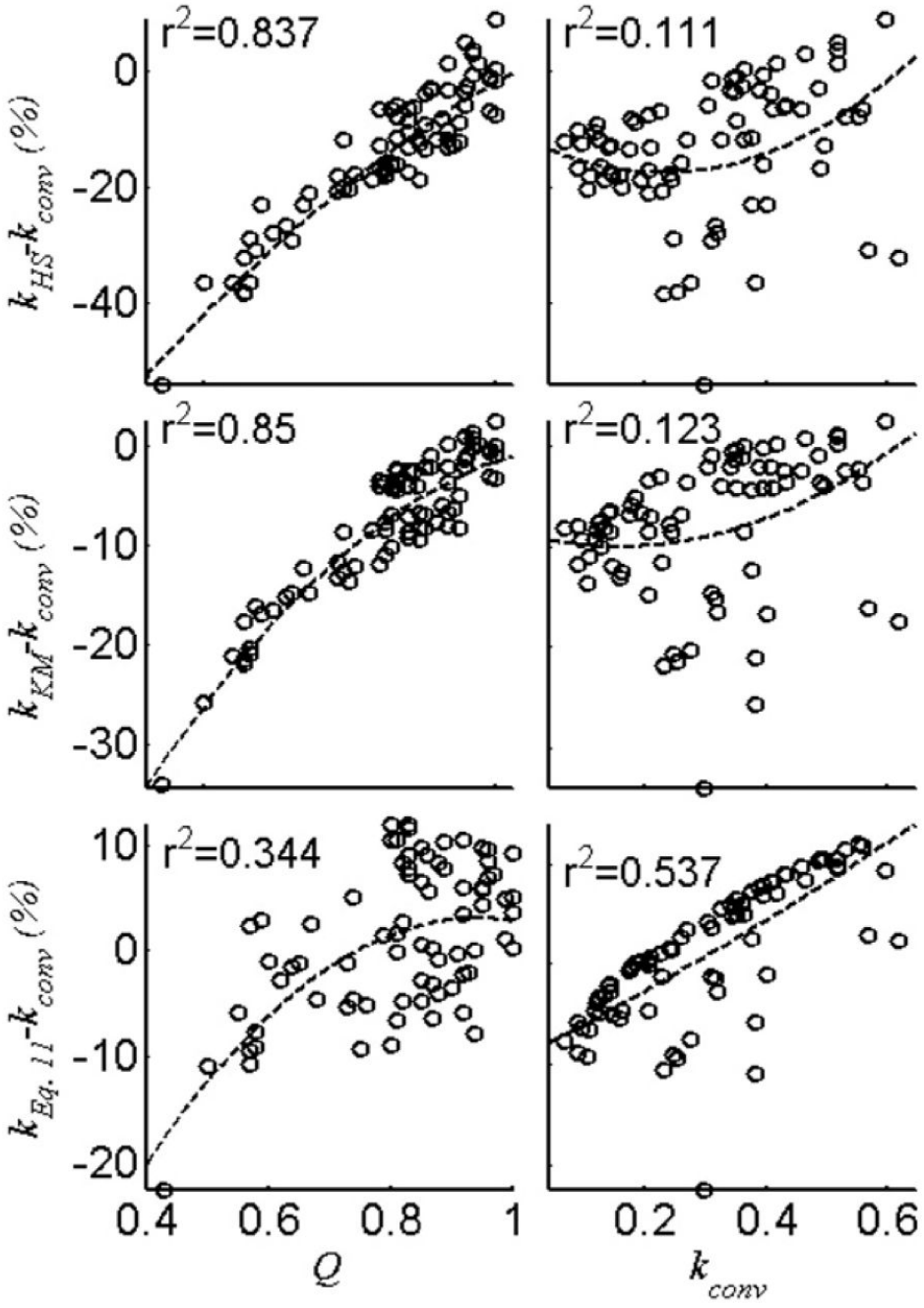

Fig. 6.

Percent adjustment made to k_{conv} by k_{HS}, k_{KM} and $k_{Eq.\ (11)}$ (using FAST* coefficients from Table 4) as a function of Q and k_{conv} for the 113 individual slice FAST data from the 14 normal controls (38 spectra) and 34 patients (75 spectra) with $Q \leqslant 1$. Best-fit second-order curves are shown (dashed line) with the coefficient of determination, r^2.

Table 1

Notation used in the saturation-transfer experiment for measuring the reaction rate constant between two moieties A and B

Symbol	Meaning
M_{0A}, M_{0B}	Equilibrium magnetization of A and B in absence of irradiation and chemical exchange
A_n, B_n	Equilibrium magnetization of A and B in presence of chemical exchange
A_s, B_s	Equilibrium magnetization of A and B in the presence of chemical exchange and selective irradiation of B
A_c, B_c	Equilibrium magnetization of A and B in the presence of chemical exchange and selective irradiation of the control site
Q	Irradiation spillover quality index: $Q = A_c/A_n$
T_{1A}, T_{1B}	The longitudinal relaxation time of A and B in the absence of irradiation and chemical exchange
T_{1A}^{sat}	The apparent longitudinal relaxation time of A in the presence of chemical exchange and selective irradiation of B

Table 2

Parameters of the two sites of the CK reaction used in simulations

Parameter	Min	Max
M_{0A} (PCr)	0.5	2
M_{0B} (γ-ATP)	1	1
T_{1A} (s)	4.4	6.5
T_{1B} (s)	2	2
T_{2A} (s)	0.1	0.1
T_{2B} (s)	0.05	0.05
ω_A (rad s^{-1})	0	0
ω_B (rad s^{-1})	440	440
ω_1 (rad s^{-1})	15.7	62.8

Table 3

Coefficients of the correction polynomials used in Eq. (10) for the progressive saturation and the FAST experiments

Protocol	Polynomial	a_1	$a_2 a_3$
Progressive saturation	P_k	1.000	−0.403 0.046
	P_ω	−48.067	10.035−0.5951
FAST	P_k	1.000	0.225−0.005
	P_ω	−48.403	6.857−0.363

Table 4

Coefficients of the correction polynomials used in Eq. (11) for the progressive saturation and FAST experiments with $0.05 \leqslant k \leqslant 1.0$ and $0.1 \leqslant k \leqslant 0.5$ (FAST*)

Protocol	Polynomial	a_1	a_2	a_3
Progressive saturation	P_k	1.000	−0.120	−0.022
	P_Q	−2.475	3.685	−1.426
FAST	P_k	1.000	0.135	−0.007
	P_Q	−6.443	11.972	−5.712
FAST*	P_k	1.0000	−0.0534	−0.0534
	P_Q	0.2025	0.0098	−0.2585

Table 5

Means ± SD and range (min, max) of the percentage errors in the estimated *k* calculated by different correction methods

Correction method	Percent error in *k*, mean (bias) ± SD (min, max)		
	Progressive saturation	FAST	FAST*
Conventional, Eq. (3)	7.4 ± 16.0 (−17.9, 70.0)	−5.8 ± 13.4 (−29.3, 39.7)	−1.5 ± 7.4 (−17.0, 27.3)
HS, Eq. (4)	−13.9 ± 15.2 (−35.6,−3.4)	−14.6 ± 16.2 (−33.7,−1.8)	−14.3 ± 15.7 (−33.5,−3.6)
KM, Eq. (5)	−3.0 ± 5.1 (−18.4,4.4)	−11.0 ± 12.7 (−27.3,0.8)	−8.4 ± 9.3 (−18.9,−0.7)
Numerical inversion	0.6 ± 2.6 (−12.6, 9.5)	0.2 ± 5.7 (−20.2, 29.1)	0.2 ± 4.6 (−12.8, 31.3)
Eq. (10)	1.8 ± 4.0 (−8.0, 12.3)	0.0 ± 2.2 (−10.4, 7.1)	0.1 ± 1.3 (−5.5, 3.5)
Eq. (11)	1.8 ± 5.5 (−25.5, 8.6)	−0.3 ± 3.2 (−12.8, 8.0)	0.1 ± 2.9 (−9.3, 4.7)

The errors are calculated for progressive saturation and FAST over the range of parameters listed in Table 2; for $0.05 \leqslant k \leqslant 1.0$ and for FAST with $0.1 \leqslant k \leqslant 0.5$ (FAST*).

Table 6

Effect of different correction formulae on experimental subject-averaged forward cardiac CK reaction rates *k* (means ± SD) in normal subjects

Correction method	***k* for *Q* ⩽ *1* only (*n* = *14*)**	***k* with *Q* set to *1* when *Q* >1 (*n* = *18*)**	***k* using actual *Q* (*n* = *18*)**
Conventional, Eq. (3)	0.34 ± 0.09	0.36 ± 0.07	0.36 ± 0.07
Horska–Spencer, Eq. (4)	0.31 ± 0.09[a]	0.33 ± 0.08[b]	0.34 ± 0.08
Kingsley–Monahan, Eq. (5)	0.32 ± 0.08[a]	0.34 ± 0.07[b]	0.34 ± 0.07[b]
Eq. (11) with FAST* coefficients	0.36 ± 0.10[a]	0.37 ± 0.08[a]	0.36 ± 0.08

[a] $P \leqslant 0.01$ vs conventional data in same column (2-tailed paired *t*-test).

[b] $P \leqslant 0.05$ vs conventional data in same column (2-tailed paired *t*-test).